applied sciences

MDPI

Article

A Direction-Sensitive Microwave Sensor for Metal Crack Detection

Boyang Qian [1], Liang Mou [1], Li Wu [1,*], Zelong Xiao [1], Taiyang Hu [1] and Jinwei Jiang [2]

[1] School of Electronic and Optical Engineering, Nanjing University of Science & Technology, Nanjing 210094, China
[2] School of Intelligent Control, Changzhou Vocational Institute of Industry Technology, Changzhou 213164, China
* Correspondence: li_wu@njust.edu.cn

Featured Application: Nondestructive metal crack detection, crack direction sensing.

Abstract: For metal crack nondestructive detection, most conventional crack sensors are unable to realize the crack direction detection. In this work, a direction-sensitive microwave sensor is proposed for metal crack detection. The proposed sensor consists of a rectangular patch resonator and two perpendicular coupled feeding ports, which improves the current distribution on patch surface and the sensitivity for crack direction detection. The performances of the proposed sensor are verified by simulation and measurement experiments. The results show that the width sensitivities of two feeding ports are 100 MHz/mm and 63.3 MHz/mm, respectively, and the sensitivity of the sensor for crack direction detection are 6.10 MHz/5 degrees and 1.93 MHz/5 degrees, respectively. Due to the advantages of a simple structure, low profile, large coverage area and high sensitivity, the proposed sensor has a great application potential in nondestructive detection fields.

Keywords: structural health monitoring (SHM); metal crack detection; direction-sensitive; microwave sensor

Citation: Qian, B.; Mou, L.; Wu, L.; Xiao, Z.; Hu, T.; Jiang, J. A Direction-Sensitive Microwave Sensor for Metal Crack Detection. *Appl. Sci.* **2022**, *12*, 9045. https://doi.org/10.3390/app12189045

Academic Editor: Atsushi Mase

Received: 6 August 2022
Accepted: 6 September 2022
Published: 8 September 2022

1. Introduction

Structural Health Monitoring (SHM) involves the detection and identification of damages in structure through sensors and data processing techniques, which has drawn great interest in recent years. Generally, metal materials will be corroded and damaged after long-term use, which results in metal cracks. Additionally, the existence of cracks will greatly affect the safety of the device. To realize SHM, nondestructive detection has become an important way to prevent serious accidents caused by cracks in the metal structure [1,2].

In recent years, various nondestructive detection methods for metal crack have been developed. Eddy current testing (ECT) is one of the most important techniques in nondestructive detection. A higher sensitivity is always pursued to improve the ECT probe performance, and many approaches including probe designing, coil geometry optimization, signal postprocessing, and so on have been reported in the literature [3–5]. However, eddy current testing is difficult to quantify cracks, and can only detect cracks near the surface, which makes it difficult to detect some unreachable areas. Ultrasonic testing (UT) has the ability to detect the cracks deep beneath the surface, and is suitable for long-distance detection. However, ultrasonic testing requires transmitting and receiving devices, and the signal processing process is complicated [6–8]. Optical fiber sensors (OFS) with multiple unique advantages have shown the potential to replace conventional sensors in certain applications in these decades [9–11]. For example, fiber Bragg grating (FBG) sensor is a special type of OFS. The sensitive element of the Bragg grating is contained in the fiber core, which serves as a narrow-band reflection filter. FBG sensors are suitable for detecting elastic ultrasonic waves in solid materials. An FBG can selectively reflect a part of the incident light around its central wavelength referred to as the Bragg wavelength. However, the measurement accuracy of an FBG sensing system is critical for long-term monitoring.

In the meantime, microwave sensors have the advantages of quantified detection, easy assembly, and stable detection performance. With the development of microwave technology, a great variety of microwave sensors for metal crack nondestructive detection have been proposed [12–15], such as the waveguide sensor, coaxial sensor and microstrip sensor.

Regarding the waveguide sensor, a high-sensitivity near-field waveguide sensor loaded with a dielectric resonator for metallic crack detection is demonstrated in [16]. Both the numerical and experimental results reveal that this dielectric resonator-based waveguide sensor can effectively detect cracks on a metallic surface. The maximum sensitivity for crack depth and width detection are 0.71 GHz/mm and 1.24 GHz/mm, respectively.

As for coaxial sensor, a method based on the resonance frequency shift in coaxial resonator is presented in [17] to detect metal surface cracks. Additionally, this sensor will produce a frequency shift of 2.16 GHz when detecting a 0.2 mm-wide crack. Generally, waveguide and coaxial sensors have a higher sensitivity of crack width and depth. However, both kinds of sensors are unable to detect the orientation of crack and have a higher profile.

Compared with waveguide or coaxial sensor, microstrip sensor has the advantages of low profile, light weight and easy integration. In [18], an enhanced sensor based on symmetrical split ring resonator (SSRR) functioning at microwave frequencies has been proposed for detecting and characterizing the cracked surface of the metal materials. The minimum detection limit is investigated which is around 10 μm width or depth where the minimum shift in reflected frequency is recorded at 6.2 MHz and 3 MHz for crack width and depth, respectively. In 2020, a smart coating based on the frequency selective spoof surface plasmon polaritons was introduced for submillimeter crack monitoring [19]. The achieved depth and width sensitivity are 57.5 MHz/mm and 77.5 MHz/mm, respectively. In [20], the article presents a methodology for SHM using a passive microwave sensor, which uses the signal phase shift to realize crack detection. The microstrip sensors listed above have different performances in crack detection, but all those sensors are also not sensitive to crack direction. Therefore, to solve this problem, the direction detection of metal crack will be studied and realized in this paper.

In addition, for the conventional microstrip patch sensor, there is a deficiency that the metal cracks need to be placed in the center region of a patch, because of the nonuniform current distribution. In [21], a metal crack sensor based on a highly conductive flexible graphene film is proposed. The sensor is designed based on conformal microstrip antenna composed of a flexible graphene film radiation patch and a flexible dielectric substrate. This sensor exhibited a detection sensitivity of 36.82 MHz/mm demonstrated by both experimental and simulation results. Additionally, the direction information can be reflected by the change in resonant frequency of sensor, but cannot be quantified. Due to nonuniform current distribution, the crack sensor must be arranged at the center region of the sensor patch.

To summarize, presently there are few state-of-the-art works on the crack direction detection for microwave sensors. Additionally, it is significant to improve the current distribution of microstrip patch sensor for crack detection in practical application. Aiming at these problems, a direction-sensitive microwave sensor for metal crack detection is proposed in this paper. The presented sensor employs the dual-port coupled feeding to improve the current distribution and excite vertical and horizontal polarization current, respectively. The mutually perpendicular currents mean that the proposed sensor has direction sensibility for crack detection on the metal surface. The presented sensor can avoid the disadvantage of blind region for detection, compared with single-port crack detection sensor, which is able to improve the sensibility for detecting crack direction. In this paper, various nondestructive detection methods are described and compared at first. Then, the equivalent circuit model is established to analyze the working principles of the proposed sensor, and electromagnetic simulation experiments are conducted to analyze the influence of crack's dimensions. Lastly, the proposed sensor is fabricated, and experiments are carried out to verify the simulation results. The structure of the paper is arranged as follows. The sensor design is described detailly in Section 2. Simulation studies are discussed in Section 3. Section 4 shows the experimental results of the proposed sensor. Finally, the conclusion is presented in Section 5.

2. Sensor Design

2.1. Sensor Geometry

As depicted in Figure 1, the proposed microwave sensor consists of a rectangular patch resonator and two perpendicular feeding ports. The rectangular patch resonator is excited through feeding ports to realize crack direction detection. An impedance transformation structure is inserted between the feeding port and the rectangular patch resonator to achieve an excellent impedance matching. Additionally, a coupled feeding method is applied to improve the current distribution on the patch resonator.

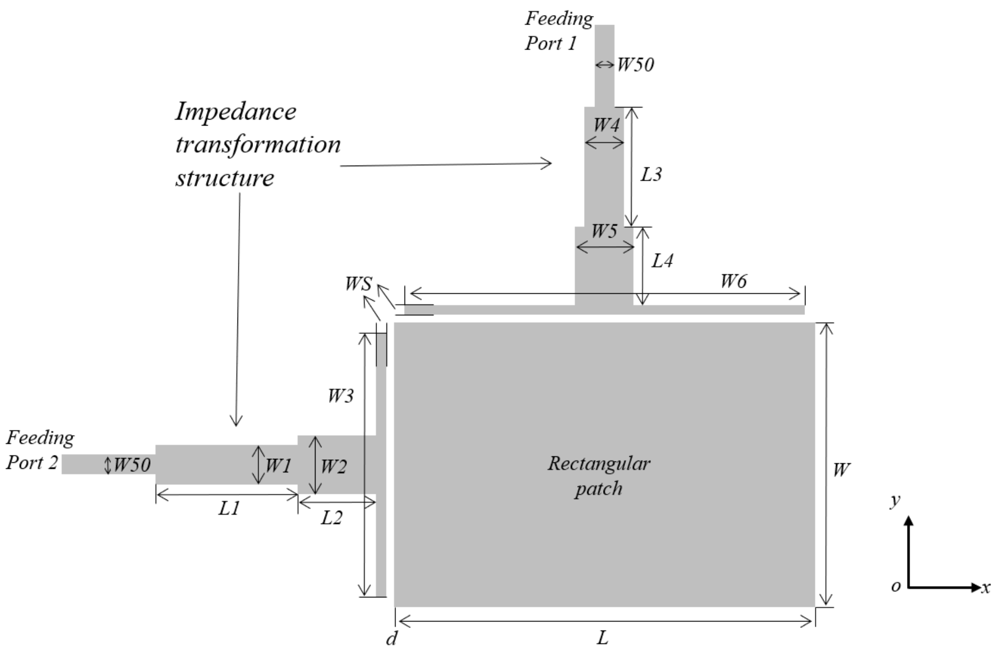

Figure 1. Geometry of the proposed direction-sensitive microwave sensor.

The designed sensor is realized with a single-layer substrate F4B (ε_r = 2.2, tan δ = 0.0037 @ 10 GHz) with a thickness of 1 mm. The operation frequency range of the proposed sensor is set from 1.5 GHz to 3 GHz after considering sensor size and fabrication cost. The length L and width W of rectangular patch shown in Figure 1 are calculated by Equations (1) and (2), which are expressed as

$$W = \frac{1}{2f_r\sqrt{\mu_0\varepsilon_0}}\sqrt{\frac{2}{\varepsilon_r+1}} = \frac{c}{2f_r}\sqrt{\frac{2}{\varepsilon_r+1}}, \tag{1}$$

$$L = \frac{1}{2f_r\sqrt{\varepsilon_{re}}\sqrt{\mu_0\varepsilon_0}} - 2\Delta L. \tag{2}$$

where, f_r is the center frequency, μ_0, ε_0 are the magnetic permeability and dielectric constant, respectively, and c is the light speed. ε_{re} is the effective dielectric constant and it can be determined with

$$\varepsilon_{re} = \frac{\varepsilon_r+1}{2} + \frac{\varepsilon_r-1}{2}\left[1+12\frac{h}{W}\right]^{-1/2}, \ W/h > 1. \tag{3}$$

Additionally, ΔL can be calculated by

$$\frac{\Delta L}{h} = 0.412 \frac{(\varepsilon_{re} + 0.3)\left(\frac{W}{h} + 0.264\right)}{(\varepsilon_{re} - 0.258)\left(\frac{W}{h} + 0.8\right)} \quad (4)$$

For the geometry shown in Figure 1, the gap distance d can be optimized to realize better impedance matching and improve the current distribution on a rectangular patch. In addition, quarter wavelength impedance matching is used to realize impedance transformation.

The specific sensor geometrical dimensions through simulation and optimization are listed in Table 1. Due to the length and width of the rectangular patch resonator being different, it will result in a resonant frequency difference between two feeding ports.

Table 1. Dimensional parameters of the proposed sensor.

Variables	Value (mm)	Variables	Value (mm)
W	40	WS	0.5
W1	5.5	W50	3
W2	6	L	50
W3	37	L1	27
W4	4.1	L2	9.3
W5	6	L3	22.4
W6	46	L4	8.8

2.2. Equivalent Circuit Model

To demonstrate the working principle of the proposed sensor, its equivalent circuit is described in this section. Figure 2a presents a physical multilayer model of the rectangular patch resonator when there is no crack on the metal ground plane.

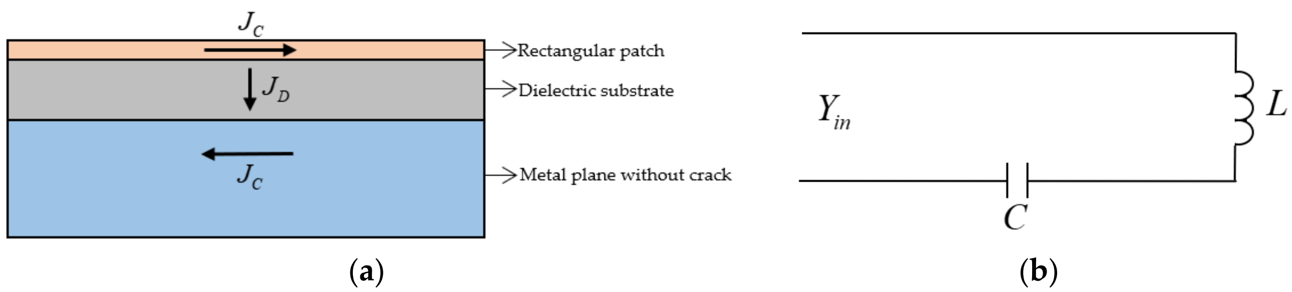

Figure 2. Equivalent model of the sensor without crack on the ground plane. (**a**) Physical model. (**b**) Equivalent Circuit.

In Figure 2a, J_D is the displacement current which is created by the electric field between the rectangular patch and ground plane, and this can be regarded as a capacitance. Additionally, the conduction current J_C, which is excited on both rectangular patch resonator and metal plane, can be considered as an inductance in the equivalent circuit. According to the physical model, the equivalent circuit of the proposed sensor can be simplified as Figure 2b shows, where L and C are the series inductance and capacitance of rectangular patch resonator, respectively. Therefore, the input admittance Y_{in} can be expressed as

$$Y_{in} = jwC + \frac{1}{jwL}. \quad (5)$$

Additionally, the reference resonant frequency f_0 of the sensor can be expressed as

$$f_0 = \frac{1}{2\pi\sqrt{LC}}. \quad (6)$$

When there is a crack on the metal ground plane, the equivalent circuit of the proposed sensor can be modeled as shown in Figure 3.

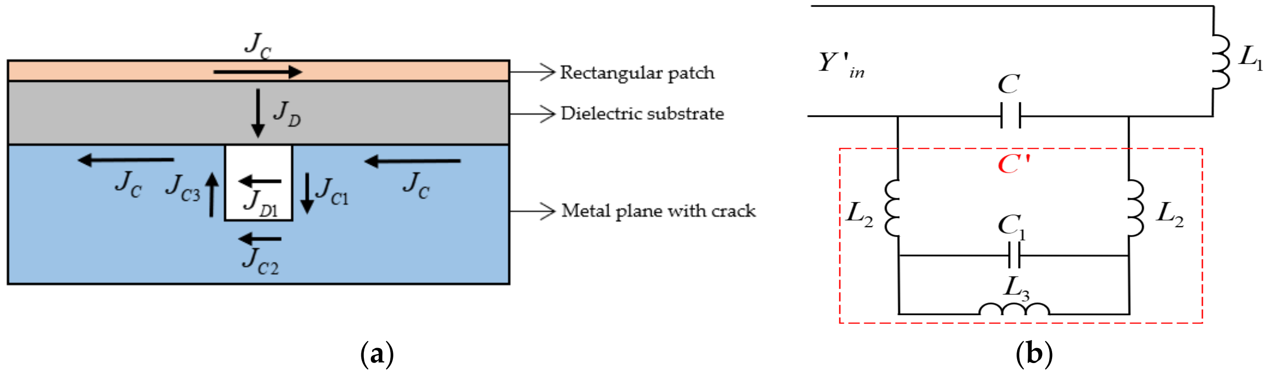

Figure 3. Equivalent model of the sensor with crack on the ground plane. (**a**) Physical model. (**b**) Equivalent Circuit.

The model presented in Figure 3a is similar to the model shown in Figure 2, in which J_D and J_C still exist.

Compared with the model in Figure 2a, it can be found that the extra conduction currents J_{C1}, J_{C2} and J_{C3} are exited along the crack boundaries except J_C due to the discontinuity on the metal ground plane. Additionally, the displacement current J_{D1} is created by the electric field between two crack boundaries where J_{C2} and J_{C3} located. So, when there is a metal crack on the metal ground plane, the additional displacement and conduction currents will introduce additional capacitances and inductances into the equivalent circuit, which can be regarded as an additional capacitance C'. The input admittance Y'_{in} of circuit can be expressed as

$$Y'_{in} = jwL + j\omega(C + C'), \tag{7}$$

where C' is the capacitance introduced by a crack, and its expression can written as

$$C' = \left(\frac{1}{\frac{1}{jwC_1 + 1/jwL_2} + jwL_1 + jwL_3} \right) / jw. \tag{8}$$

Then, the resonant frequency of the sensor for crack detection can be expressed as

$$f = \frac{1}{2\pi\sqrt{L(C + C')}}. \tag{9}$$

In summary, an additional capacitance introduced by a metal crack will lead to a decreased resonant frequency of the sensor. So, when there is a crack on the metal ground surface, the resonant frequency will deviate from the reference value. Additionally, as the capacitance C' is determined by the width, depth and direction of the metal crack, detailed characteristics of the crack can be inferred from the resonant frequency response of sensor.

2.3. Realization of Crack Direction Detection

For conventional single-port microstrip sensors, when there exists a crack parallel to the current direction, the sensors will have a blind region for crack detection and also cannot realize crack direction detection. So, a patch resonator with two feeding ports is proposed to improve the detection performances for crack detection.

Firstly, the working principle of the sensor with a single feeding port is analyzed. Figure 3 shows the schematic diagrams of the current path on the ground plane for the cases with and without a crack. When the crack on the ground plane is perpendicular to the current direction, the current path length is obviously extended, as shown in Figure 4b. However, when the crack direction is parallel to the current direction, as shown in Figure 4c, the crack has no effect on the current path length. Additionally, the resonant frequency of the sensor will not vary even though there is a crack on the ground plane. Therefore, the sensor with a single feeding port is unable to detect cracks which are parallel to the current direction.

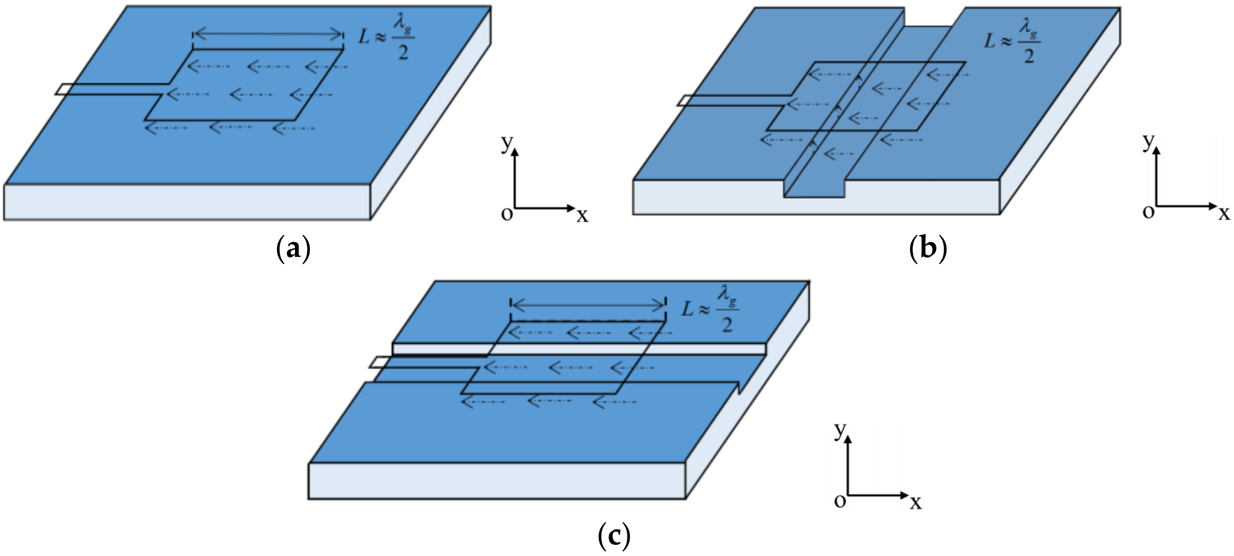

Figure 4. The current distribution of sensor with a single feeding port. (**a**) Current distribution without crack. (**b**) Current distribution with crack along oy axis. (**c**) Current distribution with crack along ox axis.

For the sensor proposed in this paper, two feeding ports are employed to generate perpendicular polarization currents which overcome the drawbacks of a single-port sensor. As shown in Figure 5, the crack parallel to the ox axis is defined as a horizontal crack, and the crack along the oy axis is denoted as a vertical crack in this paper. The horizontal and vertical cracks can be detected by analyzing the resonant frequency of Port 1 and Port 2, respectively.

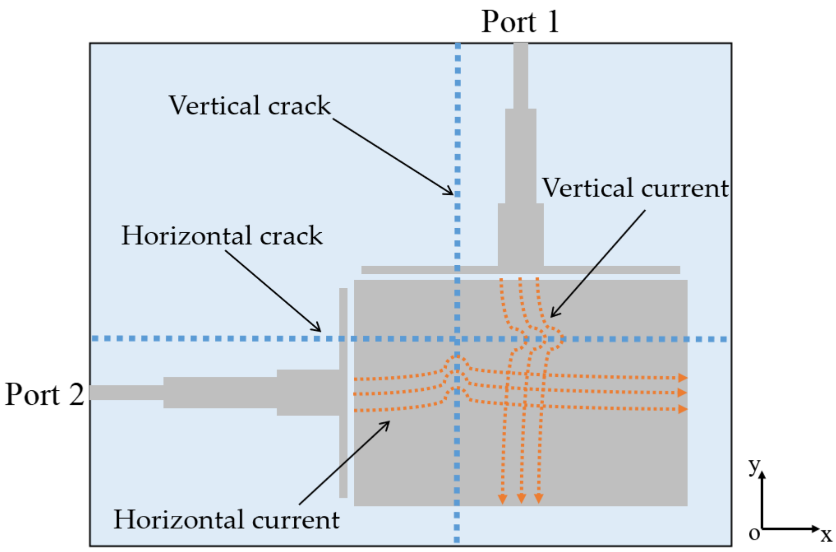

Figure 5. Crack direction detection of designed dual-port sensor.

2.4. Realization of Improved Current Distribution

As the current distribution of the rectangular patch resonator with direct feeding is limited to a narrow area, the crack occurred in the middle of the corresponding area on the metal grounding patch will have a better detection performance than the crack that occurred on the edge. So, a coupled feeding method is adopted in this paper to improve the current distribution on the patch resonator as shown in Figure 6a, and the current distribution for direct feeding is also given for the convenience to compare.

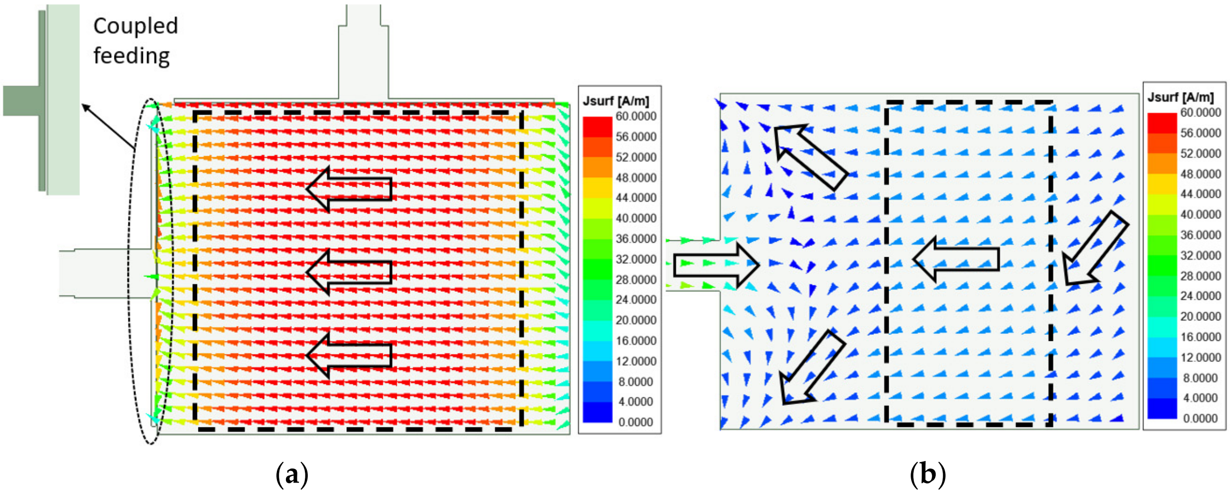

Figure 6. Current distribution of two different feeding methods. (**a**) Coupled feeding. (**b**) Direct feeding.

We can see from the simulation results that the current density of coupled feeding is much larger than that of direct feeding. Additionally, the coupled feeding has a lager coverage area with uniform current distribution. In addition, the current on the edge adjacent to the direct feeding port has a messy direction, which limits the crack detection area of the sensor. Compared with the direct feeding method, the current distribution on the resonator will be improved greatly for the coupled feeding, and this will lead to a better detection performance and a larger coverage area.

3. Simulation Study on Metal Crack Detection and Characterization

Electromagnetic simulations are performed with full-wave simulation software Ansys HFSS to verify the ability of the designed sensor for metal crack detection. Firstly, the frequency response of the sensor is simulated when there is no crack on the metal ground plane. The simulated reflection coefficient of each feeding port is shown in Figure 7. It can be found that the resonant frequency of port 1 is 2.430 GHz, while the resonant frequency of port 2 is 1.950 GHz.

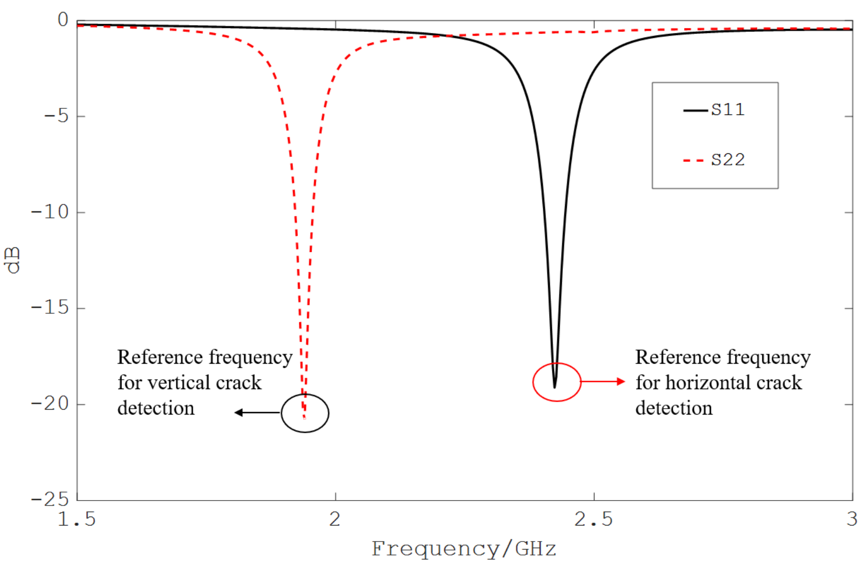

Figure 7. Simulated reflection coefficients of the sensor for the case without cracks.

Followingly, the sensor with a crack on the metal ground plane is simulated. Additionally, the influences of crack parameters such as width, depth and direction on the frequency response are also studied in the simulation.

The simulated reflection coefficients of each feeding port for vertical cracks with different widths are shown in Figure 8. It can be seen from the results that a vertical crack has little effect on the resonant frequency of port 1. Additionally, for port 2, its resonant frequency will decrease from 1.946 GHz to 1.890 GHz when the crack width increases from 0 mm to 1 mm with a step of 0.2 mm.

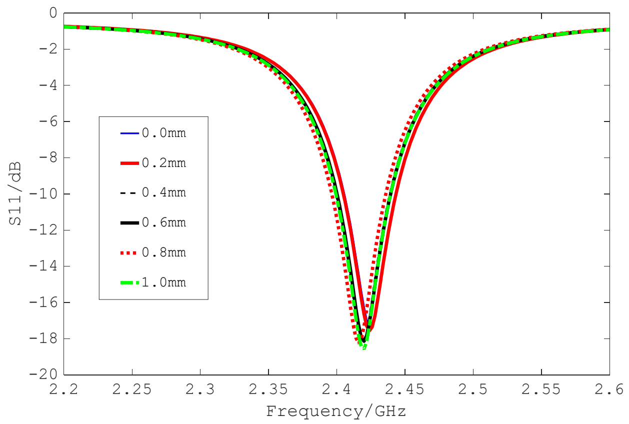

(**a**) (**b**)

Figure 8. Simulated reflection coefficients of designed sensor for vertical crack with different widths. (**a**) Port 1. (**b**) Port 2.

For the simulation results of horizontal cracks detection as presented in Figure 9, the resonant frequency of port 1 shifts from 2.426 GHz to 2.324 GHz with the crack width varies from 0 mm to 1.0 mm with a step of 0.2 mm.

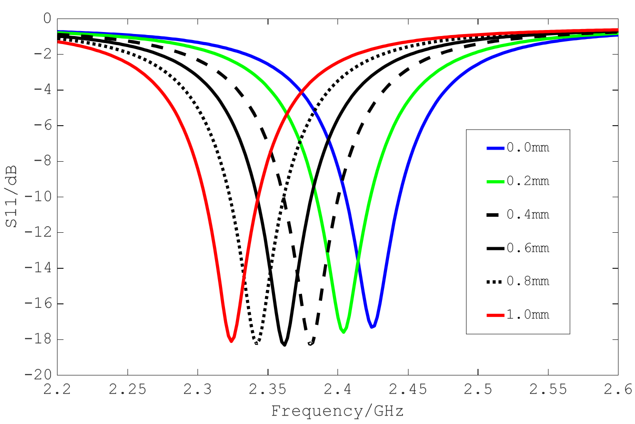

(**a**) (**b**)

Figure 9. Simulated reflection coefficients of designed sensor for horizontal crack with different widths. (**a**) Port 1. (**b**) Port 2.

The definition of crack dimension sensitivity is shown in Equation (10), Δf is the change in frequency when crack dimensions changing, and Δx is the change in crack dimensions.

$$Sensitivity = \left|\frac{\Delta f}{\Delta x}\right| \tag{10}$$

The calculated frequency sensitivity of port 1 and port 2 for crack width detection is 102 MHz/mm and 56 MHz/mm, respectively.

Then, in order to study the influence of crack depth on the resonant frequency, the depth parameter sweeps from 1.5 mm to 2.5 mm with a step of 0.5 mm and crack width is fixed at 0.4 mm. The obtained simulation results are shown in Figures 10 and 11.

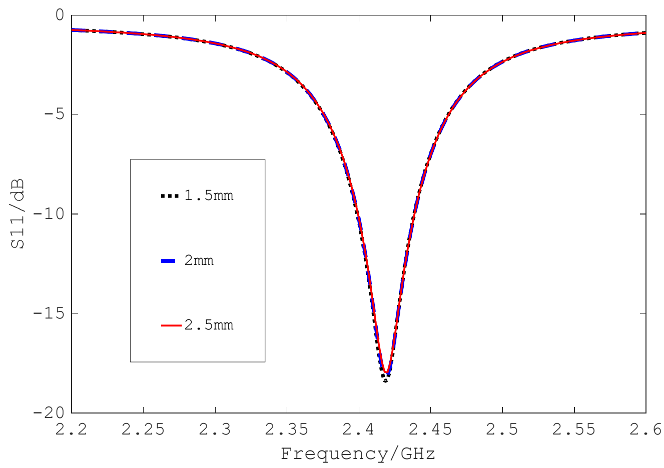

(**a**)

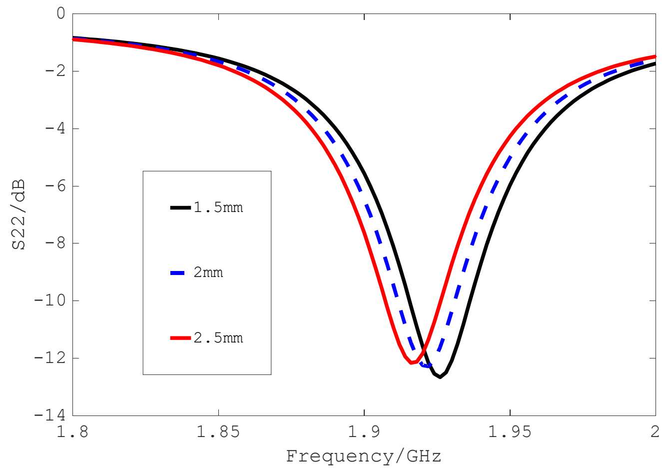

(**b**)

Figure 10. Simulated reflection coefficients of designed sensor for vertical crack with different depths. (**a**) Port 1. (**b**) Port 2.

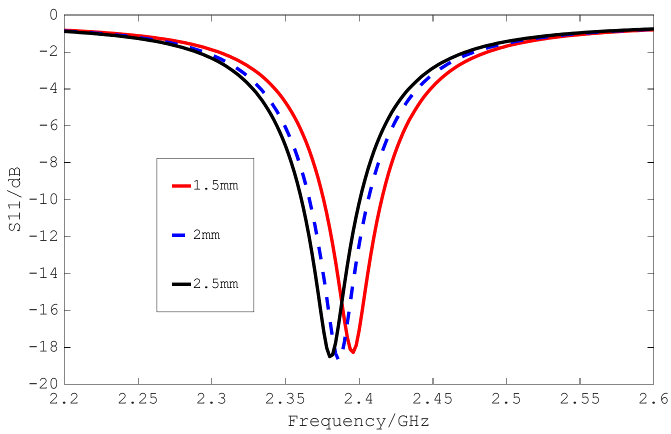

(**a**)

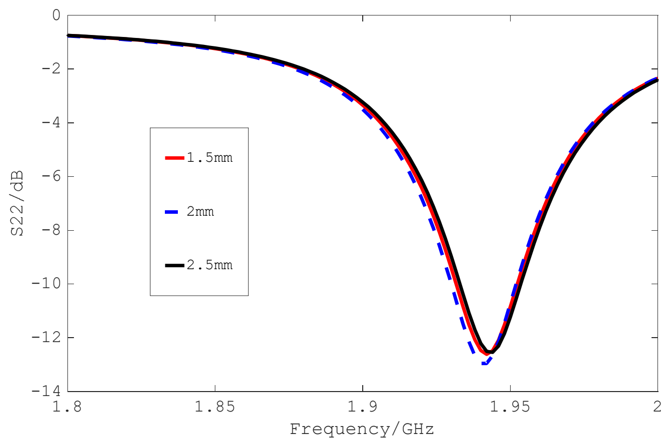

(**b**)

Figure 11. Simulated reflection coefficients of designed sensor for horizontal crack with different depths. (**a**) Port 1. (**b**) Port 2.

It can be seen from Figures 10a and 11b that the resonant frequency of each port almost keeps same while crack depth change. As can be seen from Figures 10 and 11, the resonant frequency shifts toward lower frequencies with the increase in the depths, and the sensitivity of port 1 and port 2 is 16 MHz/mm and 10 MHz/mm, respectively.

Furthermore, the sensor for crack direction detection is simulated. The depth and width of the metal crack are fixed at 2 mm and 0.6 mm, respectively, and the crack is rotated in counterclockwise direction with a step of 15 degrees (set the oy direction as 0 degrees). The simulation results of the reflection coefficient with the varying direction angle are as Figure 12 shows.

We can find that the resonant frequencies of both feeding ports vary with the crack direction. As the crack direction rotates from 0 degrees to 90 degrees, the resonant frequency of port 1 will decrease from 2.432 GHz to 2.364 GHz, while the resonant frequency of port 2 will increase from 1.896 GHz to 1.942 GHz.

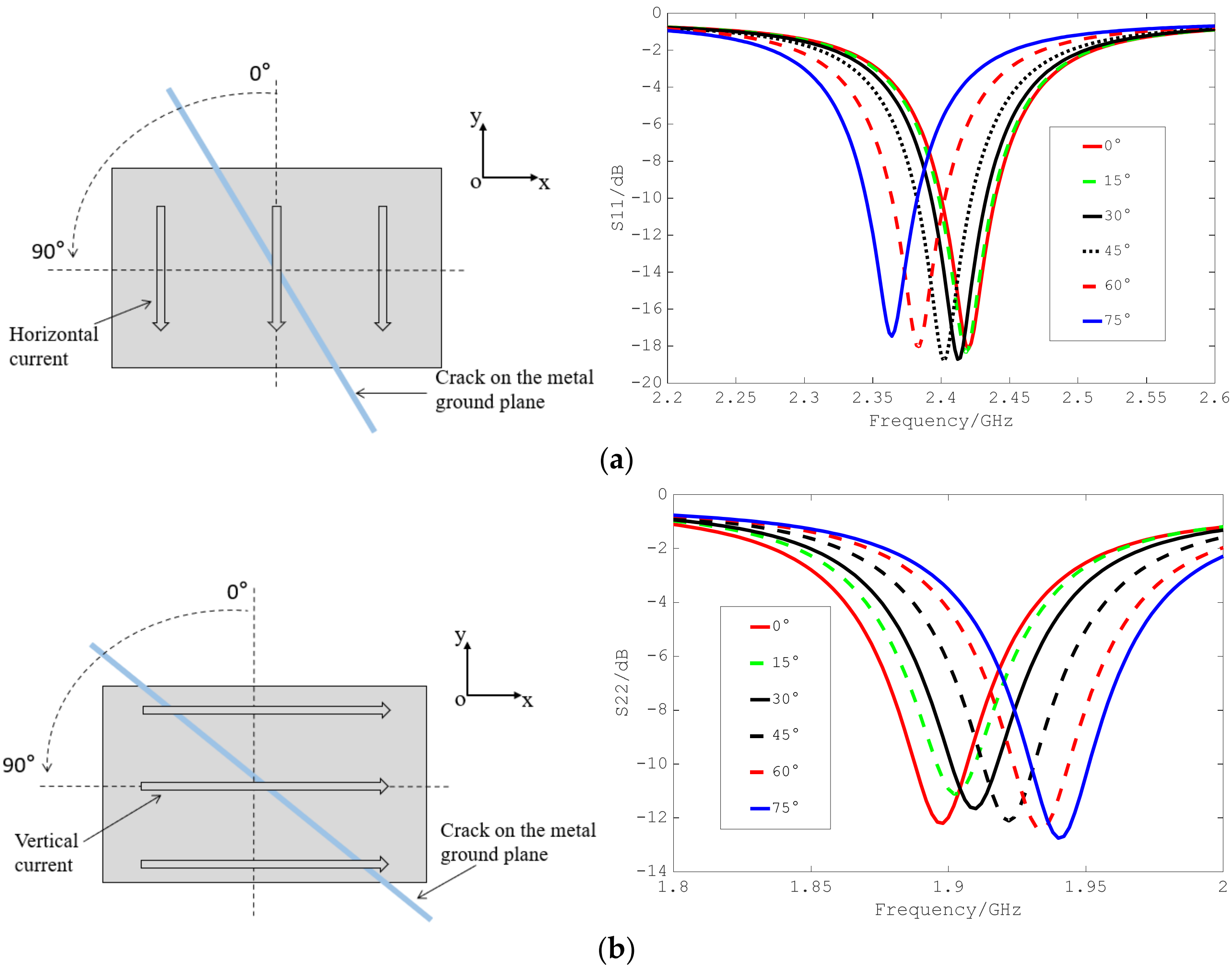

Figure 12. Simulated reflection coefficients of the designed sensor for crack with different directions. (**a**) Port 1. (**b**) Port 2.

4. Experimental Study and Discussion

To verify the performance of the proposed sensor for metal crack detection, a prototype was fabricated with the dielectric substrate of F4B. Additionally, the dielectric constant is 2.2, and the thickness is 1 mm. The fabricated sensor is illustrated in Figure 13a. Several aluminum plates are machined to generate artificial flaws to simulate real metal cracks, as presented in Figure 13b. Additionally, reflection coefficients of the fabricated sensor are measured with Keysight vector network analyzer N5244A. For scattering parameters used in the experiments, S11 is the reflection coefficient of Port 1, while S22 is the reflection coefficient of Port 2, which can be obtained by vector network analyzer (VNA).

The reflection coefficients of the fabricated sensor for crack with different parameters are measured. Figures 14 and 15 show the measurement results for the horizontal and vertical crack with a fixed depth of 2 mm and a varying width of 0.6 mm~1.2 mm.

According to measurement results, when there is no crack on the aluminum plate, the measured reference resonant frequencies of port 1 and port 2 are 2.485 GHz and 2 GHz, respectively, which correspond well to the simulation results. From Figure 15a, the resonant frequency of port 1 decreases from 2.4 GHz to 2.34 GHz when the crack width increases. Additionally, according to Figure 14b, the resonant frequency of port 2 shifts from 1.958 GHz to 1.92 GHz when the crack width increases. The sensitivity of port 1 and port 2 for crack width are 100 MHz/mm and 63.3 MHz/mm, respectively.

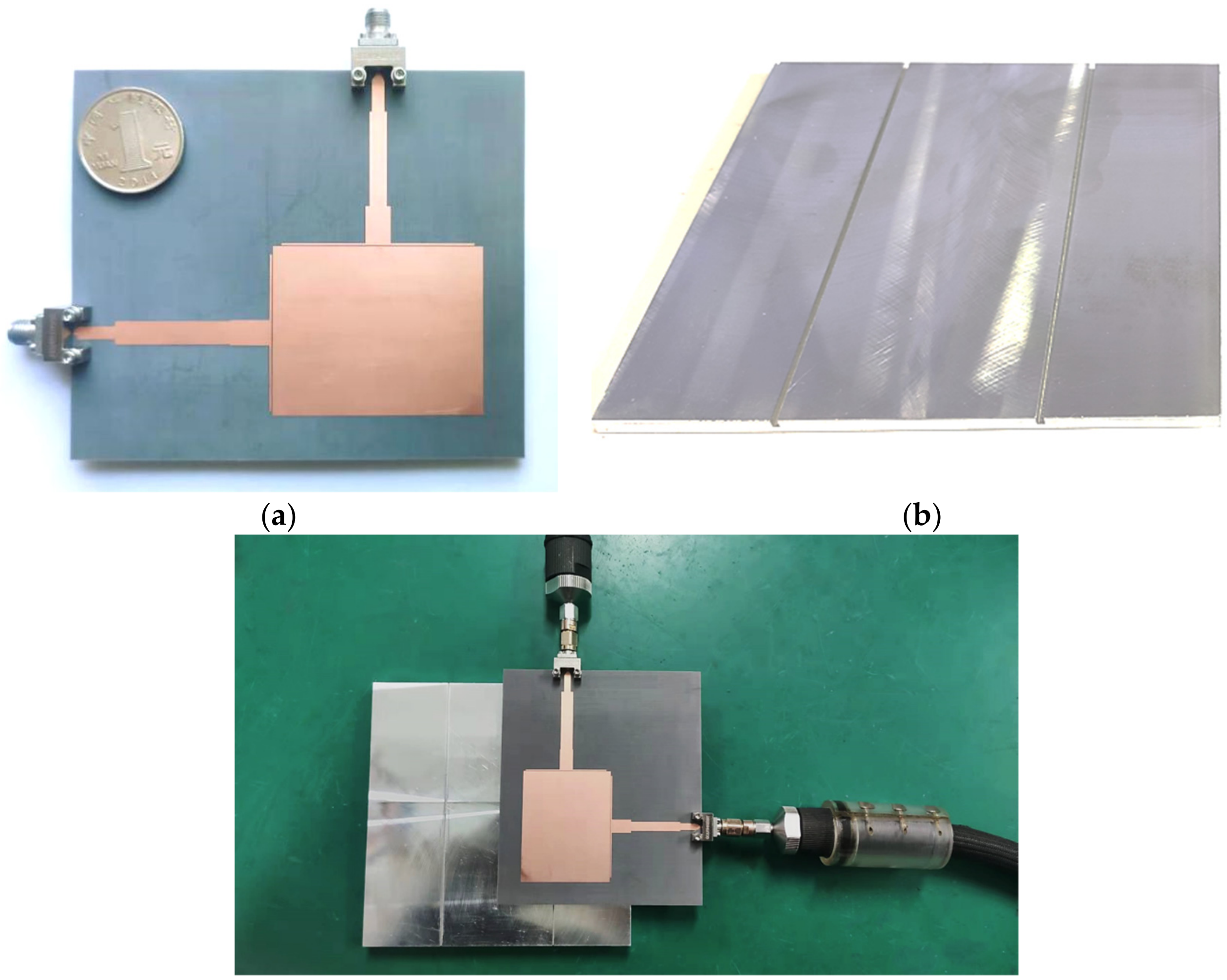

(**a**) (**b**)

(**c**)

Figure 13. Fabrication and measurement. (**a**) Fabricated sensor. (**b**) Metal crack on aluminum plate. (**c**) Reflection coefficient measurement by VNA.

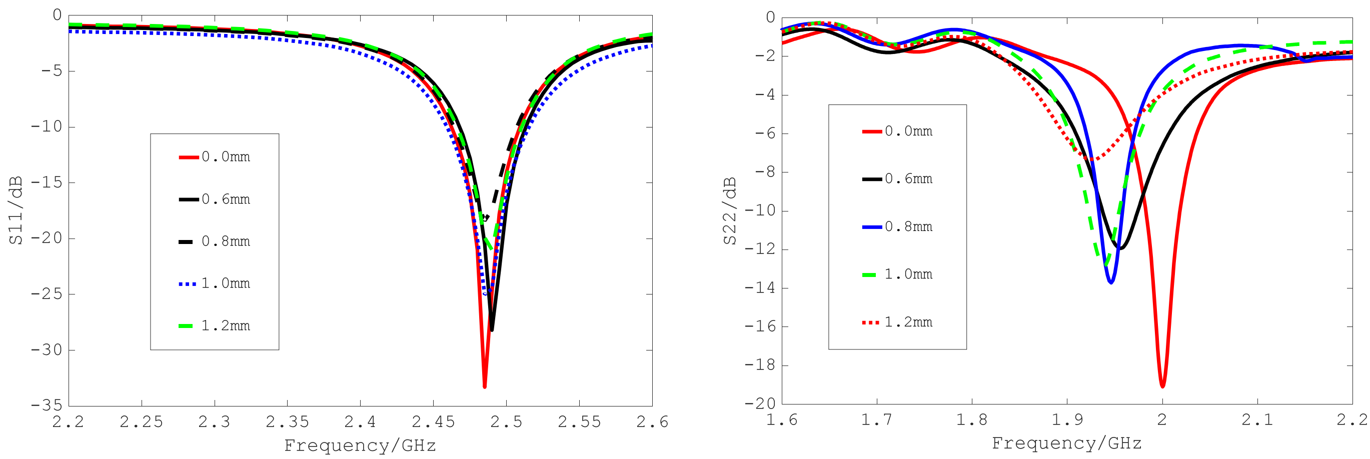

(**a**) (**b**)

Figure 14. Measured reflection coefficient results of fabricated sensor for vertical crack with different widths. (**a**) Port 1. (**b**) Port 2.

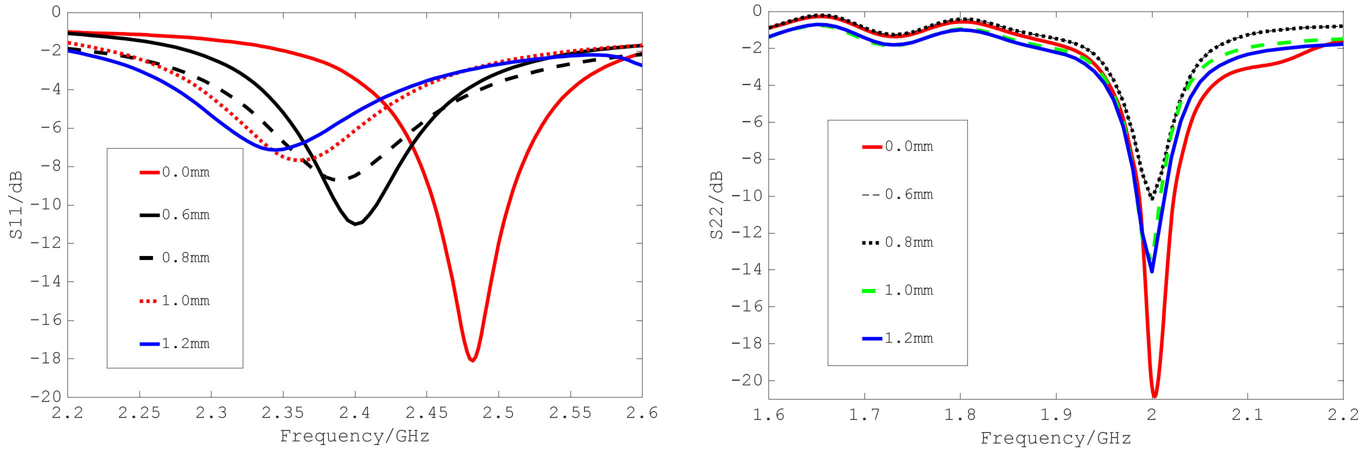

(**a**) (**b**)

Figure 15. Measured reflection coefficient results of fabricated sensor for horizontal crack with different widths. (**a**) Port 1. (**b**) Port 2.

Next, when the metal crack width is set as 0.6 mm, the measurement results at each port with different crack depths are as Figure 16 shows.

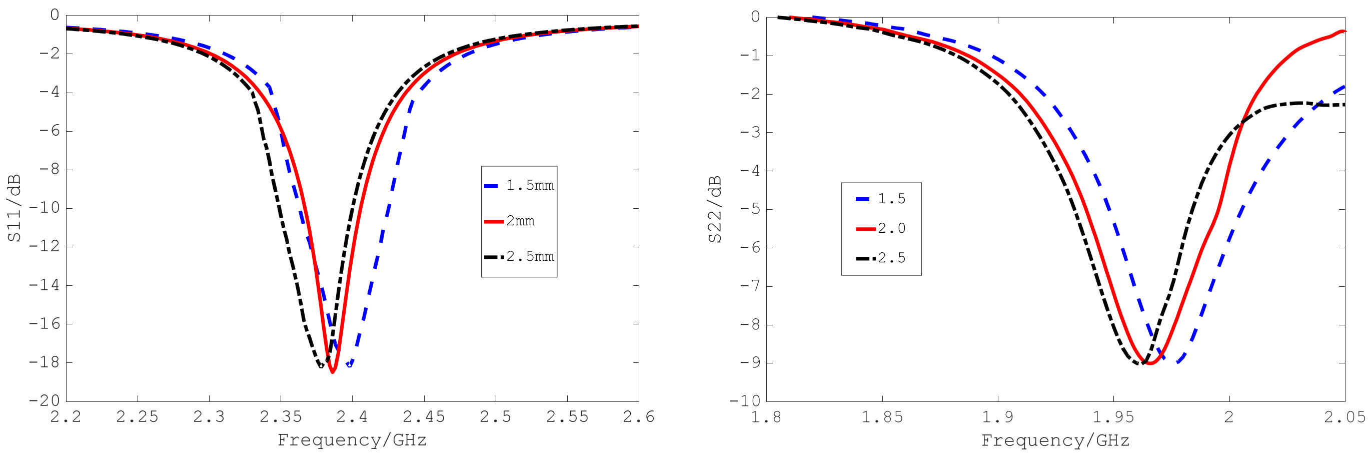

(**a**) (**b**)

Figure 16. Measured reflection coefficient results of fabricated sensor for crack with different depths. (**a**) Port 1 to horizontal cracks. (**b**) Port 2 to vertical cracks.

It can be seen that the measured resonant frequency shifts toward lower frequencies as the crack depths increase. Additionally, the sensitivity of the sensor for depth detection is about 20 MHz/mm and 14 MHz/mm for port 1 and port 2, respectively.

Then, the crack width is fixed at 0.6 mm, and the crack depth is fixed at 2 mm; the measurement results of the reflection coefficient with different crack directions are shown in Figure 17.

The measurement results show that the resonant frequency of port 1 drops from 2.491 GHz to 2.4 GHz as the crack direction angle varies from 0° to 75°, while the resonant frequency of port 2 shifts toward an opposite direction, from 1.971 GHz to 2 GHz. Additionally, the sensitivities of port 1 and port 2 for crack direction detection are 6.07 MHz/5 degrees and 1.93 MHz/5 degrees, respectively.

The results of simulation and measurement are listed in Table 2. Through comparison, the measured reference frequency and crack width detection sensitivity agree well with the simulation results. Additionally, the experimental sensitivity of crack depth detection is larger than the simulation. For the sensitivity of crack direction detection, there is a minor discrepancy between the experiment and simulation. Combing the results above, it can be concluded that the proposed sensor has a favorable performance for the crack dimensions and direction detection.

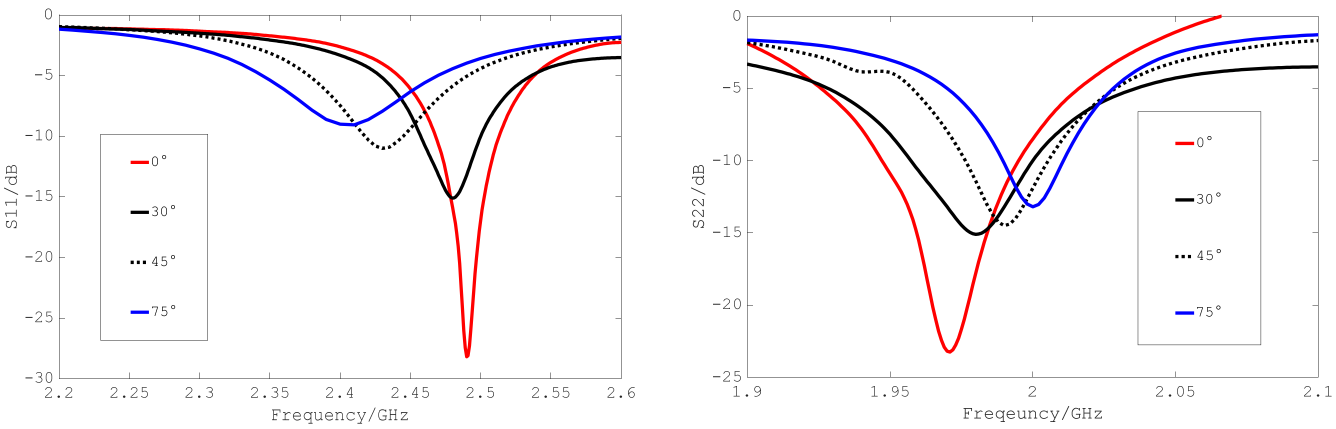

(**a**) (**b**)

Figure 17. Measured reflection coefficient results of fabricated sensor for crack with different directions. (**a**) Port 1. (**b**) Port 2.

Table 2. Comparison of results of simulation and experiment.

	Reference Frequency	Sensitivity of Crack Width (MHz/mm)	Sensitivity of Crack Depth (MHz/mm)	Sensitivity of Crack Direction Detection (MHz/5 Degrees)
Simulation results (Port 1/Port 2)	2.430/1.950	102/56	16/10	3.78/2.56
Experiment results (Port 1/Port 2)	2.485/2.000	100/63.3	20/14	6.07/1.93

Additionally, the proposed sensor is compared with other references in terms of the working frequency, sensitivity of crack width and depth, and ability of crack direction detection. The details are illustrated in Table 3.

Table 3. Comparison of different kinds of metal crack detection sensor.

	This Work	Reference [8]	Reference [10]	Reference [11]
Frequency (GHz)	2.485/2.000	4.91	4.35	2.25/3.12
Sensitivity of crack width (MHz/mm)	100/63.3	77.50	50	36.82
Sensitivity of crack depth (MHz/mm)	20/14	57.50	50	NULL
Ability of crack direction detection	YES	NO	NO	NO

Through the comparison, we can find that the sensitivity of the proposed sensor for horizontal crack width detection is the highest among listed references, and the sensitivity for vertical crack width detection is higher than that in [10,11]. It means that a larger resonant frequency shift will be contributed by the sensors with a higher sensitivity for crack detection with the same dimensions. In addition, the proposed sensor is also able to detect crack depth, though its sensitivity of crack depth is lower than sensors in [8,10]. Especially, the designed sensor has a unique ability to realize metal crack orientation detection, which other sensors cannot realize. With the ability to detect crack directions, the proposed sensor is able to avoid the blind region in crack detection and predict the crack growth direction compared with single-port sensors. In summary, the proposed sensor has the ability to detect the width, depth and direction of metal crack, and has a better comprehensive performance in crack detection than other referred sensors.

5. Conclusions

A microwave direction-sensitive sensor for metal crack detection is proposed in this paper. The proposed sensor adopts two feeding ports to obtain perpendicular polarization currents, which realize the direction detection. In addition, the orientation of metal cracks can be determined by combining the resonant frequencies of two feeding ports. Additionally, compared with the direct feeding method, a coupled feeding method is proposed in the design to improve the current distribution on the patch resonator surface, and this results in a better detection performance. Due to the advantages of a simple structure, low profile, large coverage area and high sensitivity, the proposed sensor has great application potential in nondestructive detection fields. Future work will concentrate on the conformal microstrip sensor with flexible material for the cracks occurring on irregular metal plates. Furthermore, the detection performance of irregular cracks will be studied in future work.

Author Contributions: Conceptualization, L.W.; investigation, L.M.; project administration, Z.X.; supervision, T.H.; validation, B.Q.; writing—original draft, B.Q.; writing—review and editing, L.W. and J.J. All authors have read and agreed to the published version of the manuscript.

Funding: This research was funded by Science and Technology on Near-Surface Detection Laboratory (Grant No TCGZ2017A005).

Institutional Review Board Statement: Not applicable.

Informed Consent Statement: Not applicable.

Conflicts of Interest: The authors declare no conflict of interest.

References

1. Ajgaonkar, A.; Vichare, S.; Badgujar, R.; Bansode, M.; Karia, D.; Bambole, A. Remote Structural Health Monitoring. In Proceedings of 2020 International Conference on Convergence to Digital World-QuoVadis (ICCDW), Mumbai, India, 18–20 February 2020.
2. Salim, A.; Naqvi, A.H.; Pham, A.D.; Lim, S. Complementary Split-Ring Resonator (CSRR)-Loaded Sensor Array to Detect Multiple Cracks: Shapes, Sizes, and Positions on Metallic Surface. *IEEE Access* **2020**, *8*, 151804–151816. [CrossRef]
3. Yuan, F.; Yu, Y.; Liu, B.; Tian, G. Investigation on Velocity Effect in Pulsed Eddy Current Technique for Detection Cracks in Ferromagnetic Material. *IEEE Trans. Magn.* **2020**, *56*, 1–8. [CrossRef]
4. Li, X.; Tian, G.; Li, K.; Wang, H.; Zhang, Q. Differential ECT Probe Design and Investigation for Detection of Rolling Contact Fatigue Cracks With Different Orientations. *IEEE Sens. J.* **2022**, *22*, 11615–11625. [CrossRef]
5. Gong, Z.; Yang, S. Metamaterial-Core Probes for Nondestructive Eddy Current Testing. *IEEE Trans. Instrum. Meas.* **2021**, *70*, 1–9. [CrossRef]
6. Wang, Y.; Han, S.; Yu, Y.; Qi, X.; Zhang, Y.; Lian, Y.; Bai, Z.; Wang, Y.; Lv, Z. Numerical Simulation of Metal Defect Detection Based on Laser Ultrasound. *IEEE Photonics J.* **2021**, *13*, 1–9. [CrossRef]
7. Xie, Y.; Chen, S.; Wan, X.; Tse, P.W. A Preliminary Numerical Study on the Interactions Between Nonlinear Ultrasonic Guided Waves and a Single Crack in Bone Materials With Motivation to the Evaluation of Micro Cracks in Long Bones. *IEEE Access* **2020**, *8*, 169169–169182. [CrossRef]
8. Simonetti, F.; Satow, I.L.; Brath, A.J.; Wells, K.C.; Porter, J.; Hayes, B.; Davis, K. Cryo-Ultrasonic NDE: Ice–Cold Ultrasonic Waves for the Detection of Damage in Complex-Shaped Engineering Components. *IEEE Trans. Ultrason. Ferroelectr. Freq. Control.* **2018**, *65*, 638–647. [CrossRef] [PubMed]
9. Wu, Q.; Wang, R.; Yu, F.; Okabe, Y. Application of an Optical Fiber Sensor for Nonlinear Ultrasonic Evaluation of Fatigue Crack. *IEEE Sens. J.* **2019**, *19*, 4992–4999. [CrossRef]
10. Jinachandran, S.; Ning, Y.; Wu, B.; Li, H.; Xi, J.; Gangadhara Prusty, B.; Rajan, G. Cold Crack Monitoring and Localization in Welding Using Fiber Bragg Grating Sensors. *IEEE Trans. Instrum. Meas.* **2020**, *69*, 9228–9236. [CrossRef]
11. Xiong, L.; Guo, Y.; Jiang, G.; Jiang, L.; Zhou, X. Fiber Bragg Grating Displacement Sensor With High Measurement Accuracy for Crack Monitoring. *IEEE Sens. J.* **2019**, *19*, 10506–10512. [CrossRef]
12. Zhang, J.; Huang, H.; Huang, C.; Zhang, B.; Li, Y.; Wang, K.; Su, D.; Tian, G.Y. A Configurable Dielectric Resonator-Based Passive Wireless Sensor for Crack Monitoring. *IEEE Trans. Antennas Propag.* **2019**, *67*, 5746–5749. [CrossRef]
13. Albishi, A.M.; Ramahi, O.M. Microwaves-Based High Sensitivity Sensors for Crack Detection in Metallic Materials. *IEEE Trans. Microw. Theory Tech.* **2017**, *65*, 1864–1872. [CrossRef]

14. Marindra, A.M.J.; Tian, G.Y. Chipless RFID Sensor Tag for Metal Crack Detection and Characterization. *IEEE Trans. Microw. Theory Tech.* **2018**, *66*, 2452–2462. [CrossRef]
15. Genovesi, S.; Costa, F.; Borgese, M.; Dicandia, F.A.; Monorchio, A.; Manara, G. Chipless RFID sensor for rotation monitoring. In Proceedings of the 2017 IEEE International Conference on RFID Technology & Application (RFID-TA), Warsaw, Poland, 20–22 September 2017.
16. Wang, Q.; Bi, K.; Hao, Y.; Guo, L.; Dong, G.; Wu, H.; Lei, M. High-Sensitivity Dielectric Resonator-Based Waveguide Sensor for Crack Detection on Metallic Surfaces. *IEEE Sens. J.* **2019**, *19*, 5470–5474. [CrossRef]
17. Yang, X.; Wang, Z.; Su, P.; Xie, Y.; Yuan, J.; Zhu, Z. A Method for Detecting Metal Surface Cracks Based on Coaxial Resonator. *IEEE Sens. J.* **2021**, *21*, 16644–16650.
18. Alahnomi, R.A.; Zakaria, Z.; Shairi, N.A.; Mohd Yusof, Z.; Mohd Bahar, A.A.; Alhegazi, A. Detection of Surface Cracks in Metallic Materials Using an Enhanced Symmetrical Split Ring Resonator. In Proceedings of the 2019 13th European Conference on Antennas and Propagation (EuCAP), Krakow, Poland, 31 March–5 April 2019.
19. Huang, C.; Zhou, X.; Rong, K.; Cao, J.; Zhang, J.; Wang, K. Smart Coating based on Frequency-Selective Spoof Surface Plasmon Polaritons for Crack Monitoring. In Proceedings of the 2020 IEEE 3rd International Conference on Electronic Information and Communication Technology (ICEICT), Shenzhen, China, 13–15 November 2020.
20. Norouzi, M.; Masoumi, N.; Jahed, H. Nondestructive Phase Variation-Based Chipless Sensing Methodology for Metal Crack Monitoring. *IEEE Trans. Instrum. Meas.* **2021**, *70*, 1–11. [CrossRef]
21. Tong, C.; Song, R.; Guan, H.; Yang, Y.; He, D. Conformal metal crack detection sensor based on flexible graphene film antenna. *Int. J. RF Microw. Comput. Aided Eng.* **2022**, *32*, e23172. [CrossRef]